ACS Photonics
Letter
pubs.acs.org/journal/apchd5

Single Quantum Dot with Microlens and 3D-Printed Micro-objective as Integrated Bright Single-Photon Source

Sarah Fischbach,[†] Alexander Schlehahn,[†] Alexander Thoma,[†] Nicole Srocka,[†] Timo Gissibl,[‡] Simon Ristok,[‡] Simon Thiele,[§] Arsenty Kaganskiy,[†] André Strittmatter,[†,⊥] Tobias Heindel,[†] Sven Rodt,[†] Alois Herkommer,[§] Harald Giessen,[‡] and Stephan Reitzenstein*[,†]

[†]Institute of Solid State Physics, Technische Universität Berlin, Hardenbergstraße 36, 10623 Berlin, Germany

[‡]4th Physics Institute and Research Center SCoPE and [§]Institute for Applied Optics and Research Center SCoPE, University of Stuttgart, Pfaffenwaldring 57, 70569 Stuttgart, Germany

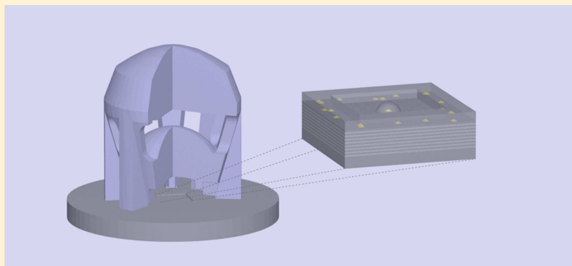

ABSTRACT: Integrated single-photon sources with high photon-extraction efficiency are key building blocks for applications in the field of quantum communications. We report on a bright single-photon source realized by on-chip integration of a deterministic quantum dot microlens with a 3D-printed multilens micro-objective. The device concept benefits from a sophisticated combination of in situ 3D electron-beam lithography to realize the quantum dot microlens and 3D femtosecond direct laser writing for creation of the micro-objective. In this way, we obtain a high-quality quantum device with broadband photon-extraction efficiency of $(40 \pm 4)\%$ and high suppression of multiphoton emission events with $g^{(2)}(\tau = 0) < 0.02$. Our results highlight the opportunities that arise from tailoring the optical properties of quantum emitters using integrated optics with high potential for the further development of plug-and-play fiber-coupled single-photon sources.

KEYWORDS: *single-photon source, 3D lithography, 3D direct laser writing, semiconductor quantum dot, micro-objective*

Advanced nanofabrication techniques have led to substantial progress in the development of solid-state-based single-photon sources.[1] Self-assembled semiconductor quantum dots (QDs) are of particular interest, as they allow for the generation of single-photon states with strong suppression of multiphoton events[2−4] and almost ideal photon indistinguishability.[4−6] Beyond that, advanced schemes of quantum computation[7−9] and communication benefit from quantum light sources that emit entangled photon pairs.[10−14] Such quantum light states can be generated via the biexciton−exciton (XX−X) radiative cascade in QDs.[15−17] Broadband photon extraction is needed to harvest such photon pairs, which usually have emission energies separated by the biexciton binding energy of typically a few millielectronvolts.[18] In addition, the far-field emission pattern needs to be shaped to match acceptance angles of different light-collecting optics. For instance, the emission profile of a single-photon source has to be optimized in order to provide high coupling efficiency to low-NA optical fibers in practical quantum devices.[3,19,20]

The combination of a QD with a DBR backside mirror and a monolithic lens was recently shown to serve as a broadband single-photon source,[2] with an extraction efficiency of up to 29% for collection optics with a numerical aperture (NA) of 0.4.[21] Here, the extraction efficiency η is limited by the rather moderate directionality of emission of the QD microlens, which leads to a strong NA dependence of η. This is of particular importance in the case of optical fibers with intrinsically small NA. As a consequence, it limits the performance of the standard microlens concept as sources for fiber-based quantum communication. This issue can be overcome by the on-chip combination of a QD microlens with a high-NA micro-objective as detailed in this Letter.

Here, we report on the realization of an efficient and broadband single-photon source fabricated by combining in situ electron-beam lithography (EBL) and optical 3D laser writing. The device is based on a single InGaAs QD that is deterministically integrated into a GaAs microlens by in situ EBL on top of a back-side distributed Bragg reflector (DBR). It is combined with a multilens micro-objective aligned and written with sub-micrometer accuracy to the microlens by means of 3D femtosecond direct laser writing.[22−26] In this way, we achieve a high-quality quantum light source with broadband extraction efficiency of up to 40% and excellent quantum optical properties in terms of multiphoton suppression associated with $g^{(2)}(\tau = 0) < 0.02$. Our results emphasize the high potential of integrated micro-optics to enhance the performance of quantum-light sources. In the future it could enable direct fiber coupling of quantum emitters in practical and stand-alone single-photon sources.

Received: March 16, 2017
Published: May 31, 2017

DOI: 10.1021/acsphotonics.7b00253
ACS Photonics 2017, 4, 1327−1332

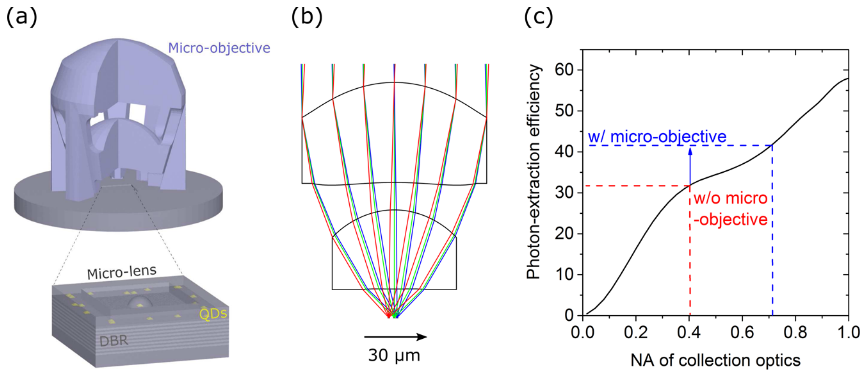

Figure 1. (a) Schematic view of the QD microlens/micro-objective device and (b) calculated ray propagation of the micro-objective with Zemax (different colors depict centered (blue) and off-centered positions of the microlens to demonstrate the field of view). (c) Calculated photon-extraction efficiency η_S of a QD microlens as a function of the numerical aperture (NA) of the collection optics. The vertical and horizontal lines mark two scenarios of different NAs. A standard QD microlens (dashed red lines) corresponds to $\eta_S^{w/o}(0.4) = 0.31$, whereas a combined microlens/micro-objective device (dashed blue lines) is calculated to result in $\eta_S(0.4) = 0.41$ by adapting the NA of 0.7, which enhances η_S by about 30%.

DEVICE DESIGN AND FABRICATION

To implement the microlens/micro-objective concept visualized in Figure 1a and b, we first optimized the QD microlens by using numerical simulations with a finite-element solver[27] in terms of maximizing the calculated extraction efficiency η_S. Maximum photon-extraction efficiency at our target wavelength of $\lambda = 930$ nm is obtained for a hemispherical lens with a base width of 2400 nm and a height of 420 nm. Figure 1c displays the corresponding calculated photon-extraction efficiency as a function of the NA of the collection optics. While obtaining η_S values of up to 60% for NAs close to unity, there is a strong decrease of η_S for numerical apertures below 0.4. Going beyond the basic microlens concept and exploiting enhanced light collection by a high-NA micro-objective, the effective collection efficiency of the combined microlens/micro-objective device will be significantly increased. The expected effect is illustrated in Figure 1c, which demonstrates that the integrated objective should enhance the extraction efficiency by about 30% from $\eta_S(0.4) = 31\%$ (dashed red lines) to $\eta_S(0.7) = 41\%$ (dashed blue lines). The expected improvement would be even more significant when considering light collection by an optical fiber, which usually has an NA of 0.2 to 0.3 in the multimode and 0.1 to 0.2 in the single-mode case. Here, a microlens/micro-objective device together with an optimized lens design for mode matching between device and fiber will be very beneficial. If the basic QD microlens was already mode-matched to the fiber, Figure 1c would predict an additional enhancement by a factor of 2 to 10 for the microlens/micro-objective device (depending on the actual NA of the fiber). We note that in the present proof-of-principle work we optimized the QD microlens and the multilens micro-objective independently, mainly because of numerical limitations. The QD microlens was optimized for light collection by an external macroscopic objective with an NA of 0.4, and the micro-objective was supposed to collect light from an isotropic point source with conversion into a collimated beam. Hence, we expect that η can be further enhanced beyond the reported values by optimizing the *combined* QD microlens/micro-objective system while taking into account the characteristics of the external light collection optics.

On the basis of these theoretical considerations we implement our device concept using self-organized InGaAs QDs as single-photon emitters. The respective sample was grown by metal−organic chemical vapor deposition on a GaAs(001) substrate. A single layer of InGaAs QDs with an areal density of 10^8 cm^{-2} was positioned 67 nm above a DBR composed of 23 pairs of $\lambda/4$-thick $Al_{0.9}Ga_{0.1}As$/GaAs layers. Finally, the QDs were capped by a 420 nm thick GaAs layer to provide material for the monolithically integrated microlenses in the subsequent nanofabrication process. This process is based on in situ electron-beam lithography, which we use to deterministically integrate single, preselected QDs into microlenses. The process includes low-temperature cathodoluminescence spectroscopy to identify suitable QDs in combination with 3D low-temperature EBL to write lens-shaped structures into AR-P 6200 (CSAR 62) as low-temperature electron-beam resist.[28] In the final step, the lens shapes are transferred into the 420 nm thick GaAs capping layer by inductively coupled plasma reactive-ion etching. A scanning-electron microscopy image of a microlens is shown in Figure 2a. We refer to ref 2 for more details on the microlens fabrication process.

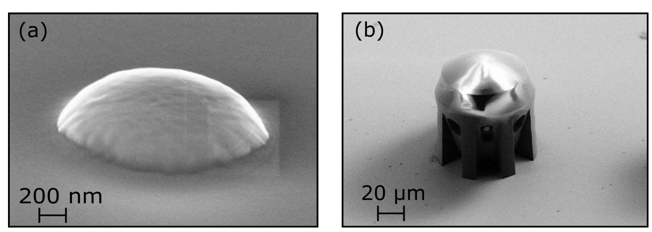

Figure 2. Scanning electron microscope images of (a) a QD microlens and (b) the fully processed QD microlens/micro-objective device.

The device processing continues with the on-chip integration of high-NA micro-objectives precisely aligned with the patterned QD microlenses. In the present work we use micro-objectives formed by a double lens system, which allow us to collect light within an NA of 0.7 and to direct it to the collection optics. We designed the lens system by using geometrical optics via the ray-tracing software Zemax (see Figure 1b) and assumed the QD to act as an ideal point source. In the optimum design the use of four aspherical surfaces allows us to achieve the targeted NA of 0.7. The design also provides a significant field of view of approximately 30 μm (see Figure 1b), which simplifies the alignment between the micro-objective and the QD microlens. To realize the micro-objectives, we apply 3D femtosecond direct laser writing based on two-photon absorption.[22−26] While this appealing

DOI: 10.1021/acsphotonics.7b00253
ACS Photonics 2017, 4, 1327−1332

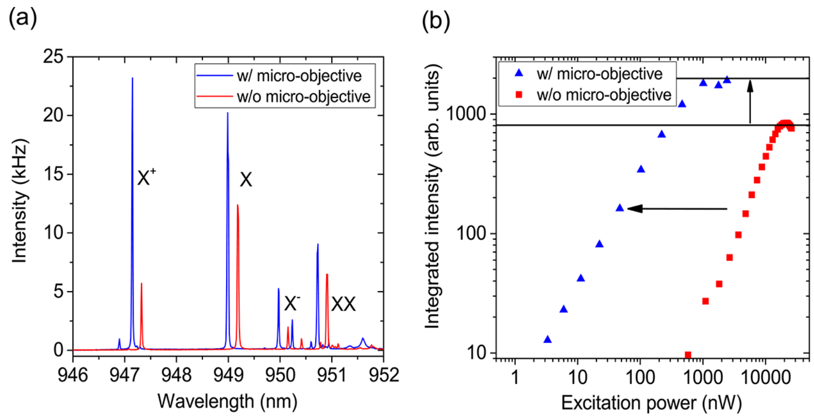

Figure 3. (a) μPL spectra of a standard QD microlens (red trace) and QD microlens/micro-objective device (blue trace). (b) Integrated intensity (sum of X, X^+, and X^-) of a standard QD microlens (red trace) and QD microlens/micro-objective device (blue trace) versus excitation power.

technique has already been used for around two decades,[29,30] only recent advances in resolution[31] have paved the way for the fabrication of sub-micrometer accurate free-form optics. For instance, the integration on LED chips[32] and manufacturing of multilens structures on the tip of a fiber[24] demonstrated the wide range of possible applications of this technique. Here, it was conducted by focusing a femtosecond laser with a wavelength of 780 nm into a UV-sensitive photoresist applied on the sample. The photoresist is polymerized via two-photon absorption at 390 nm in a small volume element around the laser focus, resulting in sub-micrometer resolution. By moving the focus in a computer-controlled fashion through the photoresist, arbitrary shapes can be written, which after the development process are forming the optical system. The high resolution makes this method suitable for the fabrication of high-quality optical elements and their accurate alignment with respect to our microlens. Figure 2b depicts a scanning electron microscopy picture of the final device.

RESULTS AND DISCUSSION

Device characterization was performed by means of micro-photoluminescence (μPL) spectroscopy at 10 K under continuous wave (cw) and pulsed excitation (f = 80 MHz) with a laser emitting at a wavelength of 671 nm. A microscope objective with an NA of 0.4 was used to collect the emission, which was spectrally dispersed by a monochromator and detected by a Si charge-coupled device camera with an overall spectral resolution of 25 μeV. To evaluate the photon-extraction efficiency η_M under pulsed optical excitation, the emission was detected using single-photon counting modules with a timing resolution of 350 ps. For this configuration, we determined a setup efficiency of $\eta_{setup} = (2.5 \pm 0.3) \times 10^{-3}$ according to ref 33.

Figure 3a displays a μPL spectrum (red trace) of a typical QD microlens before processing of the micro-objective. The relevant emission lines are identified as neutral exciton X at a wavelength of 949.2 nm, the charged states X^+ at 947.3 nm and X^- at 950.2 nm, and the biexciton XX at 950.9 nm by polarization and excitation-power-dependent μPL measurements. In order to determine the extraction efficiency of the QD microlens, we summed up the intensities of these three excitonic complexes in saturation and obtained $\eta_M^{w/o} = (17 \pm 2)\%$. This value is somewhat lower than expected from theory and as compared to 23% as reported in ref 2, which could be related to a slight lateral displacement of the QD with respect to the center of the microlens, resulting in lower values for η (see ref 2).

Next, we study the combined microlens/micro-objective device based on the same QD microlens as discussed above. For a better comparison we present the spectra before and after fabrication of the micro-objective jointly in Figure 3a, each recorded at the saturation pump power of the excitonic states. Both traces show the same spectral fingerprint except for a blue-shift by about 0.2 nm in the case of the fully processed microlens/micro-objective device. All excitonic lines exhibit a significant increase in count rates after application of the micro-objective, where the X^+ line exhibits the largest emission intensity and the strongest relative increase of intensity when compared to the other excitonic lines. The latter indicates a change in excess carriers at the QD position. The blue-shift can be attributed to an altered strain configuration due to the micro-objective and its posts around the microlens. A similar effect was observed for a 3D-printed solid-immersion lens above a QD[26] and for intentionally applied compressive strain via a near-field optical fiber probe.[34]

The overall extraction efficiency was determined as described above for the reference structure without micro-objective and considers again the summed intensity of X, X^+, and X^- at saturation. In comparison to the results without a micro-objective the photon-extraction efficiency has increased strongly by a factor of 2.3 to a record value of $\eta_M = (40 \pm 4)\%$, clearly outperforming the maximum value of η_M = 29% obtained for a bare QD microlens.[21] This result is in very good agreement with the simulated efficiency of 41% for an NA of 0.7 of the collection optics as shown in Figure 1c. Interestingly, the relative increase of η_{ext} is much larger than expected. This could indicate that the combined microlens/micro-objective device is more tolerant with respect to a lateral misalignment of the QD in the microlens, which possibly limited $\eta_M^{w/o}$ in the reference measurement without a micro-objective. This assumption is supported by two more QD microlens/micro-objective devices (not shown here). For those the basic QD–microlens performance was rather poor due to a presumably larger misalignment between mircrolens and QD. However, the increase in extraction efficiency after addition of the micro-objective amounted to factors of 2.4 and 3.1, respectively, which correspond very well to the previously reported value of 2.3.

A further attractive aspect of the microlens/micro-objective concept relates to its light-focusing capabilities. This leads to a more efficient excitation of the QD, as demonstrated in Figure

DOI: 10.1021/acsphotonics.7b00253
ACS Photonics 2017, 4, 1327–1332

3b, which displays the excitation power dependence of the sum intensity (of X, X^+, and X^- emission) of the QD microlens with and without a micro-objective. Apart from the increase of emission intensity as reported above, the required saturation pump power is reduced by more than one order of magnitude by adding the micro-objective, an effect that we attribute to the combined focusing effect of the micro-objective and the objective of the μPL setup. This specific feature could be particularly attractive for coherent nonlinear spectroscopy,[35] as the local excitation is more efficient. Also, resonance fluorescence experiments might benefit from the in principle lower amount of laser stray light when less incident laser power is required. Whether the additional surfaces of the multilens system diminish this positive effect by introducing more scatter sites has to be identified experimentally. In the future, antireflection coatings on the microlenses could reduce possible scattering effects.

Finally, we address the quantum nature of the emission of our microlens/micro-objective device. For this purpose the sample is analyzed with a fiber-coupled Hanbury-Brown and Twiss setup (temporal resolution: 350 ps), which is equipped with a wavelength-tunable Ti:sapphire laser providing picosecond light pulses at a repetition rate of 80 MHz. This configuration allows us to demonstrate the quantum nature of emission by measuring the second-order photon autocorrelation function. We applied pulsed wetting-layer excitation at λ = 850 nm at an excitation power of P = 87 nW, leading to saturation of the X^+ line. Figure 4 presents the measured

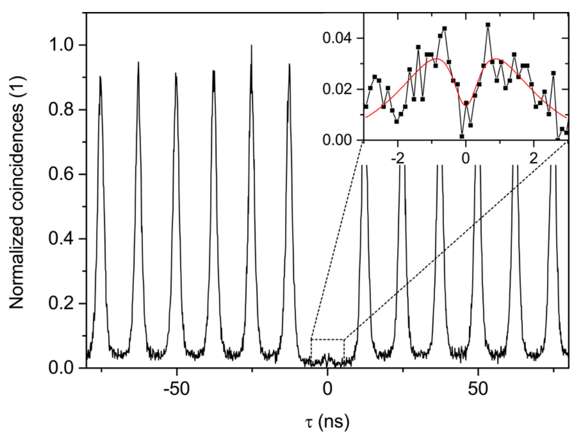

Figure 4. Photon autocorrelation measurement of a QD microlens/micro-objective device in saturation of the X^+ transition under pulsed excitation (f = 80 MHz, λ = 850 nm). The inset depicts a zoom-in of $g^{(2)}(\tau)$ and a fit (red trace) corresponding to eq 1.

histogram for the second-order photon autocorrelation function $g^{(2)}(\tau)$. The central peak at $\tau = 0$ almost vanishes, demonstrating strong suppression of multiphoton emission events. To determine the multiphoton suppression relevant for practical applications, we compare the integrated area of the central peak A_0 with the average area $\overline{A}$ of all peaks at $\tau \neq 0$. With $g^{(2)}(0)_{\text{area}} = \frac{A_0}{\overline{A}} = 0.082 \pm 0.002$ we clearly demonstrate the single-photon emission of our source. The $g^{(2)}(\tau = 0)$ itself is smaller than 0.02, as extracted from the inset of Figure 4. This inset also gives more insight into the limiting factor for $g^{(2)}(0)_{\text{area}}$. Indeed, the central dip at zero delay together with the characteristic maxima of $g^{(2)}(\tau)$ at small delays clearly indicates that the nonideal suppression of multiphoton emission is related to recapture of charge carriers and subsequent emission of photons. The underlying mechanism can be explained by additional charge carriers, which are created by the nonresonant excitation and remain in wetting layer states or are captured by charge traps.[36,37] These states repopulate the QD after the initial emission event with characteristic time delay τ_{cap}.[38] The subsequent decay with a time constant τ_{dec} results in a secondary photon emission, which explains the correlation counts for small delay times. Taking this process into account, we are able to describe the experimental $g^{(2)}(\tau)$ for small $|\tau| < 3$ ns on the basis of ref 39

$$g^{(2)}(\tau) = \exp\left(\frac{-|\tau|}{\tau_{\text{dec}}}\right) - \exp\left(\frac{-|\tau|}{\tau_{\text{cap}}}\right) \tag{1}$$

and fitting leads to $\tau_{\text{cap}} = (0.78 \pm 0.05)$ ns and $\tau_{\text{dec}} = (0.85 \pm 0.06)$ ns (see red trace in the inset of Figure 4). On the basis of this analysis we anticipate further improved values of $g^{(2)}(0)_{\text{area}}$ by applying resonant excitation, which should reduce the detrimental impact of recapture processes.

SUMMARY AND OUTLOOK

In summary, we efficiently combined two advanced 3D lithography techniques to gain a high-performance single-photon source with high extraction efficiency and very good quantum optical properties. The on-chip integrated micro-objective effectively collects emission from the QD microlens, which results in an overall photon-extraction efficiency of (40 ± 4)% into the external collection optics with an NA of 0.4. At the same time, an excellent single-photon purity is maintained and the required excitation power is decreased by one order of magnitude. The presented work demonstrates an appealing technology for NA-optimized transfer of quantum light from a single semiconductor QD into external optics. We expect that further optimization of our concept, by using micro-objectives with NAs close to unity, will make it a very promising approach for realizing highly efficient fiber-coupled single-photon sources. In combination with a compact Stirling cryocooler[40] this could pave the way toward bright and user-friendly stand-alone single-photon sources.

AUTHOR INFORMATION

Corresponding Author

*E-mail: stephan.reitzenstein@physik.tu-berlin.de.

ORCID

Simon Ristok: 0000-0001-6334-4183

Tobias Heindel: 0000-0003-1148-404X

Stephan Reitzenstein: 0000-0002-1381-9838

Present Address

⊥Otto von Guericke University Magdeburg, Universitätsplatz 2, 39106 Magdeburg, Germany.

Notes

The authors declare no competing financial interest.

ACKNOWLEDGMENTS

We acknowledge support from project EMPIR 14IND05 MIQC2 (the EMPIR initiative is cofunded by the European Union's Horizon 2020 Research and Innovation Programme and the EMPIR Participating States), from the European Research Council under the European Union's Seventh Framework ERC Grant Agreement No. 615613, and from project FI-SEQUR, which is funded by the European Regional

DOI: 10.1021/acsphotonics.7b00253
ACS Photonics 2017, 4, 1327−1332

Development Fund (EFRE) of the European Union in the framework of the program to promote research, innovation, and technologies (Pro FIT). Moreover, we thank Deutsche Forschungsgemeinschaft (DFG) for funding through SFB 787 "Semiconductor Nanophotonics: Materials, Models, Devices" and the German Federal Ministry of Education and Research (BMBF) for support through the VIP-project QSOURCE (Grant No. 03 V0630). The group from University of Stuttgart thanks ERC (Complexplas), BMBF (Printoptics and Print-function), IQST and SFB TRR21, and BW-Stiftung (Spitzen-forschung II and Opterial) for support.

■ REFERENCES

(1) Aharonovich, I.; Englund, D.; Toth, M. Solid-state single-photon emitters. *Nat. Photonics* **2016**, *10*, 631−641.

(2) Gschrey, M.; Thoma, A.; Schnauber, P.; Seifried, M.; Schmidt, R.; Wohlfeil, B.; Krüger, L.; Schulze, J. H.; Heindel, T.; Burger, S.; Schmidt, F.; Strittmatter, A.; Rodt, S.; Reitzenstein, S. Highly indistinguishable photons from deterministic quantum-dot microlenses utilizing three-dimensional in situ electron-beam lithography. *Nat. Commun.* **2015**, *6*, 7662.

(3) Claudon, J.; Bleuse, J.; Malik, N. S.; Bazin, M.; Jaffrennou, P.; Gregersen, N.; Sauvan, C.; Lalanne, P.; Gérard, J.-M. A highly efficient single-photon source based on a quantum dot in a photonic nanowire. *Nat. Photonics* **2010**, *4*, 174−177.

(4) Somaschi, N.; et al. Near-optimal single-photon sources in the solid state. *Nat. Photonics* **2016**, *10*, 340−345.

(5) Wei, Y.-J.; He, Y.-M.; Chen, M.-C.; Hu, Y.-N.; He, Y.; Wu, D.; Schneider, C.; Kamp, M.; Höfling, S.; Lu, C.-Y.; Pan, J.-W. Deterministic and Robust Generation of Single Photons from a Single Quantum Dot with 99.5% Indistinguishability Using Adiabatic Rapid Passage. *Nano Lett.* **2014**, *14*, 6515−6519.

(6) Thoma, A.; Schnauber, P.; Gschrey, M.; Seifried, M.; Wolters, J.; Schulze, J.-H.; Strittmatter, A.; Rodt, S.; Carmele, A.; Knorr, A.; Heindel, T.; Reitzenstein, S. Exploring Dephasing of a Solid-State Quantum Emitter via Time- and Temperature-Dependent Hong-Ou-Mandel Experiments. *Phys. Rev. Lett.* **2016**, *116*, 033601.

(7) Kok, P.; Munro, W. J.; Nemoto, K.; Ralph, T. C.; Dowling, J. P.; Milburn, G. J. Linear optical quantum computing with photonic qubits. *Rev. Mod. Phys.* **2007**, *79*, 135−174.

(8) Gong, Y.-X.; Zou, X.-B.; Ralph, T. C.; Zhu, S.-N.; Guo, G.-C. Linear optical quantum computation with imperfect entangled photon-pair sources and inefficient non̆photon-number-resolving detectors. *Phys. Rev. A: At., Mol., Opt. Phys.* **2010**, *81*, 052303.

(9) Cai, X.-D.; Wu, D.; Su, Z.-E.; Chen, M.-C.; Wang, X.-L.; Li, L.; Liu, N.-L.; Lu, C.-Y.; Pan, J.-W. Entanglement-Based Machine Learning on a Quantum Computer. *Phys. Rev. Lett.* **2015**, *114*, 110504.

(10) Ekert, A. K. Quantum cryptography based on Bell's theorem. *Phys. Rev. Lett.* **1991**, *67*, 661−663.

(11) Briegel, H.-J.; Dür, W.; Cirac, J. I.; Zoller, P. Quantum Repeaters: The Role of Imperfect Local Operations in Quantum Communication. *Phys. Rev. Lett.* **1998**, *81*, 5932−5935.

(12) Gisin, N.; Thew, R. Quantum communication. *Nat. Photonics* **2007**, *1*, 165−171.

(13) Simon, C.; de Riedmatten, H.; Afzelius, M.; Sangouard, N.; Zbinden, H.; Gisin, N. Quantum Repeaters with Photon Pair Sources and Multimode Memories. *Phys. Rev. Lett.* **2007**, *98*, 190503.

(14) Mower, J.; Zhang, Z.; Desjardins, P.; Lee, C.; Shapiro, J. H.; Englund, D. High-dimensional quantum key distribution using dispersive optics. *Phys. Rev. A: At., Mol., Opt. Phys.* **2013**, *87*, 062322.

(15) Benson, O.; Santori, C.; Pelton, M.; Yamamoto, Y. Regulated and Entangled Photons from a Single Quantum Dot. *Phys. Rev. Lett.* **2000**, *84*, 2513−2516.

(16) Moreau, E.; Robert, I.; Manin, L.; Thierry-Mieg, V.; Gérard, J. M.; Abram, I. Quantum Cascade of Photons in Semiconductor Quantum Dots. *Phys. Rev. Lett.* **2001**, *87*, 183601.

(17) Stevenson, R. M.; Young, R. J.; Atkinson, P.; Cooper, K.; Ritchie, D. A.; Shields, A. J. A semiconductor source of triggered entangled photon pairs. *Nature* **2006**, *439*, 179−182.

(18) Rodt, S.; Schliwa, A.; Pötschke, K.; Guffarth, F.; Bimberg, D. Correlation of structural and few-particle properties of self-organized InAs/GaAs quantum dots. *Phys. Rev. B: Condens. Matter Mater. Phys.* **2005**, *71*, 155325.

(19) Barnes, W. L.; Björk, G.; Gérard, J. M.; Jonsson, P.; Wasey, J. A. E.; Worthing, P. T.; Zwiller, V. Solid-state single photon sources: light collection strategies. *Eur. Phys. J. D* **2002**, *18*, 197−210.

(20) Bulgarini, G.; Reimer, M. E.; Bouwes Bavinck, M.; JÃns, K. D.; Dalacu, D.; Poole, P. J.; Bakkers, E. P. A. M.; Zwiller, V. Nanowire Waveguides Launching Single Photons in a Gaussian Mode for Ideal Fiber Coupling. *Nano Lett.* **2014**, *14*, 4102−4106.

(21) Schlehahn, A.; Gaafar, M.; Vaupel, M.; Gschrey, M.; Schnauber, P.; Schulze, J.-H.; Rodt, S.; Strittmatter, A.; Stolz, W.; Rahimi-Iman, A.; Heindel, T.; Koch, M.; Reitzenstein, S. Single-photon emission at a rate of 143 MHz from a deterministic quantum-dot microlens triggered by a mode-locked vertical-external-cavity surface-emitting laser. *Appl. Phys. Lett.* **2015**, *107*, 041105.

(22) Schell, A. W.; Kaschke, J.; Fischer, J.; Henze, R.; Wolters, J.; Wegener, M.; Benson, O. Three-dimensional quantum photonic elements based on single nitrogen vacancy-centres in laser-written microstructures. *Sci. Rep.* **2013**, *3*, 1577.

(23) Shi, Q.; Sontheimer, B.; Nikolay, N.; Schell, A. W.; Fischer, J.; Naber, A.; Benson, O.; Wegener, M. Wiring up pre-characterized single-photon emitters by laser lithography. *Sci. Rep.* **2016**, *6*, 31135.

(24) Gissibl, T.; Thiele, S.; Herkommer, A.; Giessen, H. Two-photon direct laser writing of ultracompact multi-lens objectives. *Nat. Photonics* **2016**, *10*, 554−560.

(25) Gissibl, T.; Thiele, S.; Herkommer, A.; Giessen, H. Sub-micrometre accurate free-form optics by three-dimensional printing on single-mode fibres. *Nat. Commun.* **2016**, *7*, 11763.

(26) Sartison, M.; Portalupi, S. L.; Gissibl, T.; Jetter, M.; Giessen, H.; Michler, P. Combining in-situ lithography with 3D printed solid immersion lenses for single quantum dot spectroscopy. *Sci. Rep.* **2017**, *7*, 39916.

(27) *JCMSuite*; JCMwave GmbH, http://jcmwave.com.

(28) Kaganskiy, A.; Heuser, T.; Schmidt, R.; Rodt, S.; Reitzenstein, S. CSAR 62 as negative-tone resist for high-contrast e-beam lithography at temperatures between 4K and room temperature. *J. Vac. Sci. Technol., B: Nanotechnol. Microelectron.: Mater., Process., Meas., Phenom.* **2016**, *34*, 061603.

(29) Maruo, S.; Nakamura, O.; Kawata, S. Three-dimensional microfabrication with two-photon-absorbed photopolymerization. *Opt. Lett.* **1997**, *22*, 132−134.

(30) Cumpston, B. H.; Ananthavel, S. P.; Barlow, S.; Dyer, D. L.; Ehrlich, J. E.; Erskine, L. L.; Heikal, A. A.; Kuebler, S. M.; Lee, I.-Y. S.; McCord-Maughon, D. Two-photon polymerization initiators for three-dimensional optical data storage and microfabrication. *Nature* **1999**, *398*, 51−54.

(31) Fischer, J.; Wegener, M. Three-dimensional optical laser lithography beyond the diffraction limit. *Laser Photon. Rev.* **2013**, *7*, 22−44.

(32) Thiele, S.; Gissibl, T.; Giessen, H.; Herkommer, A. M. Ultra-compact on-chip LED collimation optics by 3D femtosecond direct laser writing. *Opt. Lett.* **2016**, *41*, 3029.

(33) Schlehahn, A.; Thoma, A.; Munnelly, P.; Kamp, M.; Hfling, S.; Heindel, T.; Schneider, C.; Reitzenstein, S. An electrically driven cavity-enhanced source of indistinguishable photons with 61% overall efficiency. *APL Photonics* **2016**, *1*, 011301.

(34) Robinson, H. D.; Müller, M. G.; Goldberg, B. B. Local optical spectroscopy of self-assembled quantum dots using a near-field optical fiber probe to induce a localized strain field. *Appl. Phys. Lett.* **1998**, *72*, 2081.

(35) Jakubczyk, T.; Delmonte, V.; Fischbach, S.; Wigger, D.; Reiter, D. E.; Mermillod, Q.; Schnauber, P.; Kaganskiy, A.; Schulze, J.-H.; Strittmatter, A.; Rodt, S.; Langbein, W.; Kuhn, T.; Reitzenstein, S.; Kasprzak, J. Impact of Phonons on Dephasing of Individual Excitons in

Deterministic Quantum Dot Microlenses. *ACS Photonics* **2016**, *3*, 2461−2466.
(36) Peter, E.; Laurent, S.; Bloch, J.; Hours, J.; Varoutsis, S.; Robert-Philip, I.; Beveratos, A.; Lemaître, A.; Cavanna, A.; Patriarche, G.; Senellart, P.; Martrou, D. Fast radiative quantum dots: From single to multiple photon emission. *Appl. Phys. Lett.* **2007**, *90*, 223118.
(37) Kumano, H.; Harada, T.; Suemune, I.; Nakajima, H.; Kuroda, T.; Mano, T.; Sakoda, K.; Odashima, S.; Sasakura, H. Stable and efficient collection of single photons emitted from a semiconductor quantum dot into a single-mode optical fiber. *Appl. Phys. Express* **2016**, *9*, 032801.
(38) Chang, H.-S.; Chen, W.-Y.; Hsu, T.-M.; Hsieh, T.-P.; Chyi, J.-I.; Chang, W.-H. Origins of nonzero multiple photon emission probability from single quantum dots embedded in photonic crystal nanocavities. *Appl. Phys. Lett.* **2009**, *94*, 163111.
(39) Dalgarno, P. A.; McFarlane, J.; Brunner, D.; Lambert, R. W.; Gerardot, B. D.; Warburton, R. J.; Karrai, K.; Badolato, A.; Petroff, P. M. Hole recapture limited single photon generation from a single n-type charge-tunable quantum dot. *Appl. Phys. Lett.* **2008**, *92*, 193103.
(40) Schlehahn, A.; Krüger, L.; Gschrey, M.; Schulze, J.-H.; Rodt, S.; Strittmatter, A.; Heindel, T.; Reitzenstein, S. Operating single quantum emitters with a compact Stirling cryocooler. *Rev. Sci. Instrum.* **2015**, *86*, 013113.

DOI: 10.1021/acsphotonics.7b00253
ACS Photonics 2017, 4, 1327−1332